



HAL
open science

Surface Analysis Insight Note: Observations relating to photoemission peak shapes, oxidation state, and chemistry of titanium oxide films

P. Bargiela, V. Fernandez, W. Ravisy, D. Morgan, M. Richard-Plouet, N. Fairley, J. Baltrusaitis

► To cite this version:

P. Bargiela, V. Fernandez, W. Ravisy, D. Morgan, M. Richard-Plouet, et al.. Surface Analysis Insight Note: Observations relating to photoemission peak shapes, oxidation state, and chemistry of titanium oxide films. *Surface and Interface Analysis*, 2023, 10.1002/sia.7283 . hal-04393876

HAL Id: hal-04393876

<https://hal.science/hal-04393876>

Submitted on 23 Apr 2024

HAL is a multi-disciplinary open access archive for the deposit and dissemination of scientific research documents, whether they are published or not. The documents may come from teaching and research institutions in France or abroad, or from public or private research centers.

L'archive ouverte pluridisciplinaire **HAL**, est destinée au dépôt et à la diffusion de documents scientifiques de niveau recherche, publiés ou non, émanant des établissements d'enseignement et de recherche français ou étrangers, des laboratoires publics ou privés.

Surface Analysis Insight Note: Observations relating to photoemission peak shapes, oxidation state and chemistry of titanium oxide films

Pascal Bargiela,¹ Vincent Fernandez,² William Ravisy,² David Morgan,³ Mireille Richard-Plouet,² Neal Fairley⁴ and Jonas Baltrusaitis^{5*}

¹The Institute for Research on Catalysis and the Environment of Lyon (*IRCELYON*), 2 Avenue Albert Einstein, 69626 Villeurbanne, France

²Nantes Université, CNRS, Institut des Matériaux Jean Rouxel de Nanites, IMN, F-44000 Nantes, France

³Cardif Catalysis Institute, Cardiff University, Translational Research Hub, Maindy Road, Place, Cardiff CF24 4HQ, United Kingdom

and

HarwellXPS – EPSRC National Facility for Photoelectron Spectroscopy, Research Complex at Harwell (RCaH), Didcot, Oxon, OX11 0FA, United Kingdom

⁴Casa Software Ltd, Bay House, 5 Grosvenor Terrace, Teignmouth, Devon TQ14 8NE, United Kingdom

⁵Department of Chemical and Biomolecular Engineering, Lehigh University, 111 Research Drive, Bethlehem, PA 18015, USA

Abstract

XPS measurement involves recording photoemission peaks emanating from core-level electrons. These core-level electrons do not directly participate in chemical bonds but are altered by interactions with other bonding electrons within the electron configuration of an atom. It is common practice to describe the coordination of metal atoms in a binding configuration with their nearest neighbors in terms of oxidation state, a measure by which the number of electrons redistributed between atoms forming chemical bonds. In XPS terms, change to an oxidation state is commonly inferred by correlating photoemission signal with binding energy. The assumption, when classifying photoemission signals into distinct spectral shapes, is that a distribution of intensities shifted to lower binding energy is evidence of a reduction in oxidation state. In this Insight note, we raise the prospect that changes in photoemission peak shape may occur without obvious changes, determined by XPS, in stoichiometry for a material. It is well known that TiO₂ measured by XPS yields reproducible Ti 2p photoemission peaks. However, on exposing TiO₂ to ion beams, Ti 2p photoemission evolves to complex distributions in intensity, which are particularly difficult to analyze by traditional fitting of bell-shaped curves to these data. For these reasons, in this insight note, a thin film of TiO₂ deposited on a silicon substrate is chosen for analysis by XPS and linear algebraic techniques. The results from TiO₂ are used to raise the awareness that not all deformations in photoemission signal unambiguously imply a change in oxidation state. Alterations in spectral shapes created from modified TiO₂, which might be interpreted as the change in oxidation state, are assessed in terms of relative proportions of titanium to oxygen. It is found through detailed analysis

of spectra that quantification by XPS, using procedures routinely used in practice, is not in accord with the typical interpretations of photoemission shapes.

*corresponding author: job314@lehigh.edu; +1-610-758-6836

Keywords: titania; XPS; oxidation state; linear least squares; component spectra

Introduction

This *Insight* note is intended to raise awareness among XPS users about the need to correlate chemical states through fitting peak models to data with basic quantification expressing stoichiometric relationships. In an ideal world, one might expect both forms of analysis to be consistent with one another but there are situations where these two forms of analysis are contradictory. There may be good reasons why these two sources of information do not agree, but finding an explanation when agreement is not possible, is often as enlightening as when both concur.

Quantification by XPS [1], for most users, means applying a set of steps prescribed by the manufacturers of the instrument used to collect their data. These steps necessarily involve the use of relative sensitivity factors (RSFs), some form of instrumental transmission correction [2], and, depending on RSFs, some form of explicit correction for the influence of escape depth on peak intensity. Both transmission and escape depth corrections are energy dependent, meaning the intensity of photoemission peaks is dependent on the energy at which the signal is recorded, whilst the escape depth also has a material dependency [3]. Quantification obtained by following the prescribed methodology is by no means perfect [4]. However, understanding why results from quantification fall short of the expected composition can be an important step in understanding a sample. When adjusting photoemission peak intensity to produce atomic concentration or peak ratios, two correction factors of concern are: 1) the appropriateness of an escape depth correction and 2) the accuracy of the transmission correction. The former necessitates knowledge of the sample while the latter is dependent on the calibration of an instrument [5]. Since these two factors are energy dependent, their influence can be eliminated, to some extent, by selecting photoemission lines close in energy.

In this insight note, we use a film of TiO₂ deposited using PECVD on a silicon substrate [6]. The TiO₂ is assumed to be more than three attenuation lengths in thickness, which is supported by the lack of silicon signal within spectra. Given the Ti 2p and O 1s photoemission lines are close in energy (ca. 70 eV separation), we can use these two signals to determine the relative proportions of titanium and oxygen within the film without significant errors due to transmission, but more importantly, their use reduces errors due to escape depth, the influence of which alters with film thickness.

In a well-calibrated and maintained XPS instrument, the uncertainty in escape depth corrections is different from transmission correction in the sense that factors other than the kinetic energy of electrons alter signal intensity. The origin of escape depth correction is due to the attenuation of the photoemission signal caused by interactions of the photoelectron with atoms different from the atom excited by a photon. The depth within the sample, from which an electron is emitted, is limited by these inelastic scattering events, and the depth from which electrons emerge from the sample, changes with kinetic energy. Therefore, when peak intensity is corrected for escape depth, the correction is accounting for a change in volume from which electrons are sampled. Only for truly homogeneous samples can corrections of this nature be performed. Hence, correcting peak area for escape depth using corrections applied to a film thinner than three attenuation lengths (the depth from which electrons are sampled by XPS), the film thickness itself alters the true relationship between signal intensity as well as the kinetic energy of the electrons. The consequence of applying escape depth correction to films of thickness less than three attenuation lengths (without accounting for film thickness), is the composition determined from lower kinetic energy photoemission is amplified compared to photoemission measured using higher kinetic energy photoelectrons. Hence, if the need for escape depth correction is minimized, the accuracy of quantification is enhanced.

The method used to modify TiO₂ from the initial well-formed Ti⁴⁺ material is to irradiate the surface with a single-spot beam of low-energy monoatomic argon ions of 500 eV defocused to spread over a large area. The rate of change in spectral shapes, as measured by Ti 2p, is controlled by the time that the sample is exposed to the ion beam between XPS measurements. The experiment is performed in three stages. Initially, sputtering for 10 seconds between XPS cycles continued until the evolution in Ti 2p converged to a relatively constant line shape. The sputter time was then increased to 50 seconds per sputter cycle. The final stage of the experiment involved sputtering for 250 seconds per sputter cycle. Extending the sputter time produces new shapes in the Ti 2p spectra, not apparent for data collected following 10 seconds per sputter cycle.

Controlled changes to these Ti 2p spectra are a prerequisite for the analysis of data using linear algebra [7,8]. The stability of the spectra (concerning energy) during XPS and sputtering cycles is also a requirement for the analysis of these data. Thus, at each increment in time per sputter cycle, a repeat measurement was performed to ensure at each stage in the experiment the spectra, in the absence of ion beam intervention, were reproducible. These checks are important since, when spectra such as Ti 2p are observed to alter in shape, the possibility of charging effects as electrons are emitted from the sample and ions with opposite charges impact the surface may distort spectra between measurements [9,10]. Central to the analysis of these Ti 2p spectra is the acquisition of O 1s, C 1s, Ti 3p, O 2s and valence band spectra. Ti 2p, O 1s and C 1s were of importance since peak models fitted to O 1s and C 1s provided necessary information when interpreting elemental quantification. These three narrow scan spectra also served to support the assertion that charging effects in spectra were not significant to the analysis described below. Namely, evolution in the Ti 2p spectra manifested as a signal moving to lower binding energy, while the O 1s signal was relatively stable in shape with small changes predominantly to higher binding energy and C 1s attenuated in intensity but appeared to have a consistent binding energy. Ti 3p, O 2s and valence band were also included in the analysis resulting in the component spectra characteristic of different phases of TiO₂. These observations all contribute to the belief that these changes in Ti 2p spectra genuinely reflect changes in the sample and are without significant instrumental artifacts.

The analysis of these data makes use of linear algebraic methods as well as traditional nonlinear least squares fitting of peak models to data [11]. Quantification of photoemission signal is performed using the method prescribed by Kratos Analytical Ltd for data recorded on Axis Nova XPS instruments. The results, presented below, make use of linear algebra to construct, from data, component spectra with shapes characteristic of different phases of the sample throughout the experiment. These component spectra are quantified and shown to yield spectroscopic shapes that would suggest an altered oxidation-state, but relative intensities of photoemission peaks that suggest little change in stoichiometry. The question of the suitability of line shapes derived by the linear algebra is assessed by a challenge study performed by extracting the line shapes computed for Ti 2p only and applying these computed shapes to data from a second experiment conducted in a different regime from the experiment used to compute the line shapes. The second experiment involved measuring spectra along a line scan of stage movements over a surface exposed to the ion beam. Variation in spectral shapes, in this second experiment, is due to variation in ion beam flux over the large area affected.

These experiments and analyses create results for chemical states, implied by line shapes, and quantification derived from photoemission intensities, that do not support one another. The logic and analysis techniques are, therefore, presented below so that users of XPS are made aware of such anomalies in the interpretation of XPS data.

Results and Discussion

When measured from a pure TiO_2 material in a 4+ oxidation state, the characteristic of Ti 2p is amongst the simplest photoemission from metal oxides. This statement is borne out in the Ti 2p spectra shown in Figure 1a. The spectrum corresponding to the as-received surface is typical of Ti^{4+} , where photoemission results in two well-resolved peaks, possessing line shapes with Voigt characteristics [12]. There is little evidence of overlapping satellite structures often seen in other d-block metal oxide spectra [13–15], suggesting that photo-ionization of titanium in the 4+ oxidation state is well-defined in both the initial and final state for the atom in the solid state. However, the contrast between Ti 2p spectra before and after exposure to ion beam sputtering is significant. Figure 1 shows a sequence of spectra measured from TiO_2 film deposited on a silicon substrate where an ion beam has been used to modify the surface. Argon ions of energy 500 eV spread over a large area alter the surface properties, creating obvious changes to photoemission peaks, but for which shape changes in Ti 2p data are the most apparent. Following sputtering with an ion beam, the core-level peaks for 4+ titanium gain shoulders of intensity to lower the binding energy of the initial Ti 2p doublet (Figure 1a). The magnitude of these shoulders increases with each ion-beam cycle and the extent of these lower binding energy features continues to spread in energy the longer the sample is exposed to the ion-beam. Presented with evidence of this form, the assumption for most samples analyzed by XPS is these changes to the shape of a photoemission peak represent changes in stoichiometry between atoms in the sample. However, in the case of titanium, these changes in photoemission peak shape do not easily conform to this model of photoemission. Changes to Ti 2p peak shape are clear in Figure 1a, but the ratio of titanium to oxygen does not support the assumption that these photoemission peak shapes correspond to different stoichiometry. A simple quantification of the sample in terms of titanium, oxygen and carbon is available using integration regions, in which signal above a Shirley background [16] is corrected for relative sensitivity and transmission. Quantification by these means assumes a bulk homogeneous sample, which in the absence of adventitious material is valid for the TiO_2 sample used herein. Data shown in Figures 1a, 1b and 1c were used to monitor changes in elemental composition with time of the sample exposed to the ion beam. The profile plot in Figure 1e quantifies these changes in the relative proportions of elements identified in the sample. The point to observe is how the ratio of titanium to oxygen varies initially over measurement cycles for which carbon is a significant proportion of the atomic concentration. Then following the change from 10 seconds per sputter-cycle to 50 seconds per sputter-cycle, the ratio of titanium to oxygen plateaus in the Ti:O ratio equal to 1:2. Reduction of titanium would imply changes to the ratio of titanium to oxygen, which Figure 1 does not support.

The question following inspection of Figure 1e is, if the reduction in titanium has occurred, how is it possible that oxygen is retained in the sample following the breaking and forming of bonds with titanium? The element in the analysis chamber during any XPS experiment but not open to detection is hydrogen. The other element other than titanium capable of bonding with oxygen is carbon. There is little evidence in the C 1s spectra that oxygen bonded to carbon increases with sputter time, but the role played by hydrogen is difficult to assess by XPS. The only means of making a judgment about hydrogen is to analyze the oxygen signal, which can be seen in Figure 1b (O 1s) and Figure 1d (O 2s). Both O 1s and O 2s undergo little change by sputtering, so changes due to altered carbon/oxygen chemistry or hydrogen/oxygen chemistry are difficult to assess by fitting synthetic line shapes to the highly correlated data in Figure 1b. Fortunately, carbon/oxygen chemistry is available through changes to C 1s spectra (Figure 1c), which can be seen to diminish with sputter time. It is reasonable to assume hydrogen/oxygen chemistry would similarly diminish with sputter time.

The most common approach, when presented with data of the form in Figure 1a, is to fit sets of doublet synthetic peaks to spectra, which are modeled by Voigt line shapes. Each pair of synthetic peaks is interpreted as a different oxidation state of titanium. However, the data in Figure 1 are of a form suitable for an alternative analysis that makes use of all photoemission lines to compute, from data, extended line shapes to correlate photoemission from different elements. The advantage to this alternative approach is interpretations for changes that occur in Ti 2p can be viewed in the context of other photoemission lines. Therefore, rather than attempting to construct peak models using synthetic line shapes fitted by nonlinear least squares optimization, spectra in Figure 1 are transformed into spectroscopic shapes using an approach that is now described.

Changes in Ti 2p spectra in Figure 1a are characterized by analysis techniques in CasaXPS [17] involving Principal Component Analysis (PCA), linear algebraic manipulation of spectra (LAMS) and linear least squares (LLS) optimization [18]. The output from PCA is the number of distinct vectors (abstract factors (AFs)) required to properly describe all spectra shown in Figure 1, and as a by-product of identifying vectors of most significance to these data, data smoothing is achieved. Using only PCA AFs deemed to be significant, performing LLS fitting of these significant PCA AFs to data eliminates a proportion of noise from spectra [7,8]. These smoothed spectra are the input to LAMS. The process of converting spectra in Figure 1 to component spectra shown in Figure 1f is achieved by LAMS. LAMS is performed on vectors constructed from spectra, where each vector is the merged set of intensities and data bins available from Ti 2p, O 1s, C 1s, Ti 3p, O 2s and valence band spectra shown in Figure 1. LAMS involves selecting vectors constructed by these means, on a pairwise basis. For each pair of spectra, new spectral forms are constructed by subtracting one from the other in different proportions. These new spectral shapes are searched, looking for spectral shapes that offer insight into material properties. Figure 1f displays three spectral forms that emerge from an analysis of the data in Figure 1. These spectral forms are used to reconstruct data by LLS fitting these semiempirical spectral shapes to the raw data. Thus, these computed spectral forms are the input to the LLS calculation that ultimately allows the partitioning of spectra into different phases induced by sputtering TiO₂. Hence, once computed, the selected spectral forms are better described as component spectra to a model to which LLS fitting is applied. Component spectra are chosen to maintain physically acceptable shapes for all photoemission lines. Following iterations of these LAMS steps, component spectra (Figure 1f) are computed which are used to assess changes within spectra due to sputtering of TiO₂ by argon ions.

The component spectra in Figure 1f are displayed with text strings indicating the relative proportions for titanium, oxygen and carbon in the format Ti 2p₁O 1s_xC 1s_y, where the subscripts x and y are the ratio of oxygen and carbon concerning the amount of titanium. These results, calculated for each component spectrum, suggest there is an excess of oxygen relative to titanium in the first two component spectra labeled *as-received* and *Phase 1*. However, in both component spectra, a carbon signal is also present, providing a possible explanation for the excess of oxygen in the form of carbon bonded to oxygen. A key point to observe is the classical Ti 2p doublet shape is available in the *as-received* component spectrum, yet the component spectrum labeled *Phase 1* includes a signal to the lower binding energy of the *as-received* component spectrum but without any statistically significant change in the proportions of titanium and oxygen. Further, the component spectrum labeled *Phase 2*, by contrast, does not include any carbon signal, is significantly changed in shape from the *as-received* component spectrum, but yields a ratio for titanium to oxygen of 1:2. Since these component spectra fit all spectra with similar success, the partitioning of raw data into this component spectra is possible and all three component-spectra appear to yield the ratio of titanium to oxygen with stoichiometry 1:2 expected for Ti⁴⁺. Given that the sputter experiment appeared to create two obvious shifts to lower binding energy for Ti 2p, the expectation is at least two different

oxidation states were created. Thus, the exact nature of the surface following sputtering does not appear to follow the norms for XPS data analysis.

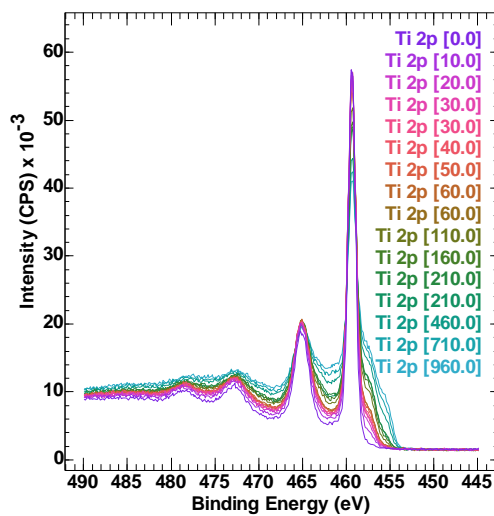
When confronted with anomalies of this nature, the first question to ask is how reproducible are these results. Therefore, a second experiment was performed to create Ti 2p spectra with similar evolution in shape but obtained by a single use of the ion beam that served two purposes. Firstly, to test the component spectra with spectra acquired under a different regime and secondly, to measure the size of the ion beam spot on the sample. Results from these analysis steps for Ti 2p component spectra are shown in Figures 2a and 2b. This second data set is formed by sputtering the sample to prepare a modified surface where the sample at different points is affected to differing degrees determined by variation in ion beam flux as a function of distance from the ion beam center. A range of photoemission Ti 2p line shapes results (Figure 2c) where the greatest change from the as-received surface Ti 2p spectrum occurs at the central position. Stage movements designed to create a line scan of XPS data ranging from the central location to a point where Ti 2p spectra return to shapes characteristic of the as-received sample result in a sequence of spectra analogous to the spectra in Figure 1a. An analysis of these Ti 2p spectra generated along a line scan is performed by extracting, from the component spectra computed using data in Figure 1, the shapes derived for Ti 2p only. These Ti 2p component spectra are shown in Figure 2a. An example of fitting a specific Ti 2p spectrum from the line scan is shown in Figure 2b. Applying fits data of the form shown in Figure 2b to all Ti 2p spectra (Figure 2c) collected along the line scan, yields the line scan of the relative peak area shown in Figure 2d, where the evolution in Ti 2p spectra as a function of position on the sample is characterized in terms of three spectral-shapes for Ti 2p. The point of demonstrating the use of component spectra calculated from data in Figure 1, applied to data in Figure 2 is that, these shapes for Ti 2p are reproducible.

Further evidence suggesting the as-received sample is compatible with a material in which titanium appears in a 4+ oxidation state is presented in Figure 3. The quantification for the same component spectra shown in Figure 1f suggests the O:Ti ratio is 2.3:1, but an analysis of the same data using Voigt line shapes to partition oxygen signal associated with titanium, from oxygen signal that predominantly is associated with carbon, demonstrates that the ratio for O:Ti in the as-received sample is better described as 2:1. Similarly, the valence band signal is offset by 3.4 eV relative to the Fermi edge for titanium metal (Figure 3c), an observation that is also compatible with titanium in a 4+ oxidation state. Thus, the component spectrum labeled Phase 2 in Figure 1f, when compared through stoichiometry, is equivalent to the as-received sample before sputtering with an ion beam. Figure 3d does suggest signal for Phase 2 is found within the band gap of TiO₂, which often is interpreted as the change in chemistry. Figure 3e compares the band structure revealed by these three component spectra in more detail. While the band structure corresponding to Phase 2 is different from the as-received TiO₂ film, the question remains whether the additional signal within the bandgap of TiO₂ is evidence of changes to bonds between titanium and oxygen, or whether such changes are due to altered physical properties of the film. The latter explanation would be consistent with the observation that stoichiometry between titanium and oxygen does not change between these three examples of component spectra. The two obvious differences highlighted by XPS are that carbon is removed and atoms have been in contact with argon ions. In this sense, these three component spectra are a product of the intervention by the ion beam. However, it has been reported previously that partial reduction of materials containing Ti⁴⁺ can be achieved by irradiation with UV light [19]. Thus, a less invasive modification to Ti⁴⁺ results in changes to the photoemission of Ti 2p and valence band signal, and does so by creating spectroscopic features similar in shape to Phase 1. It should be noted that to achieve changes to the sample leading to spectra for which the Phase 2 component spectrum is important, the required sputter cycle times twenty-five times longer than

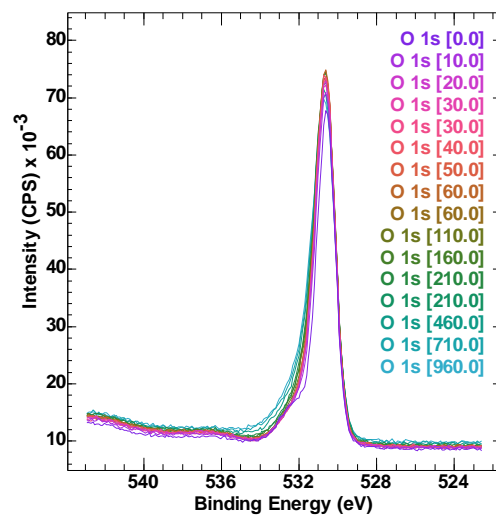
was required to create Phase 1-type shapes in spectra (Figure 3f). Based on this evidence, it would be difficult to conclude that the evolution in the shape of photoemission from titanium illustrated in Figure 1 and Figure 3f is due entirely to changes in sample oxidation states but rather is due to chemistry associated with geometric and spatial alterations between titanium and oxygen.

Conclusions

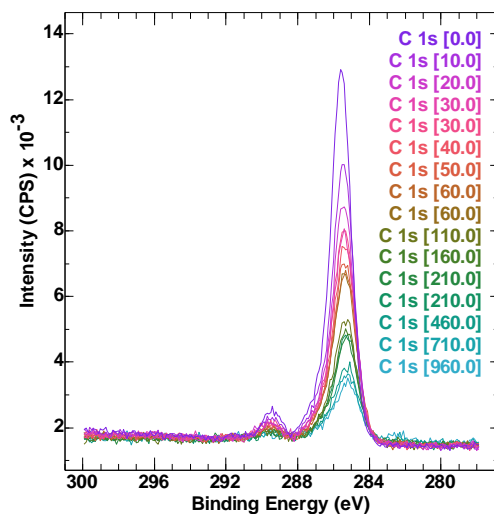
An example of a material is presented, where evolution in core-level peak shapes seems to imply a reduction in oxidation state, however, is found to be at odds with an analysis based on quantification for said material. The evidence above, presented for XPS of TiO₂ film on silicon, suggests changes in structures apparent in photoemission peaks, while reflecting alteration to sample properties, does not always imply changes in stoichiometry for a material.



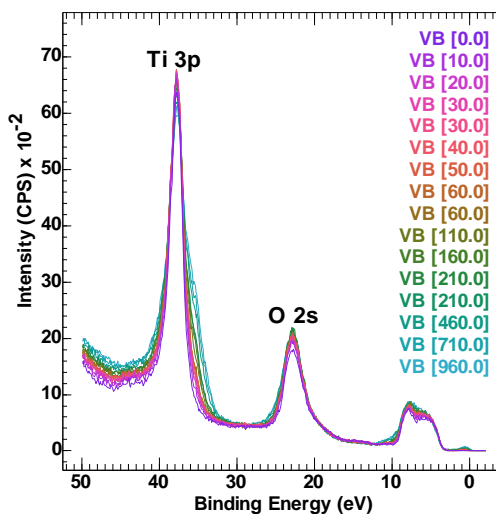
(a)



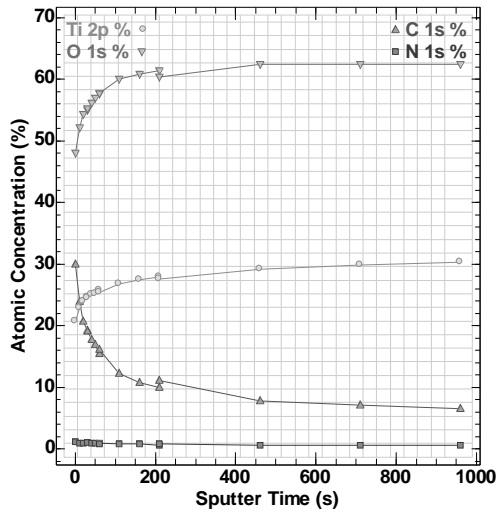
(b)



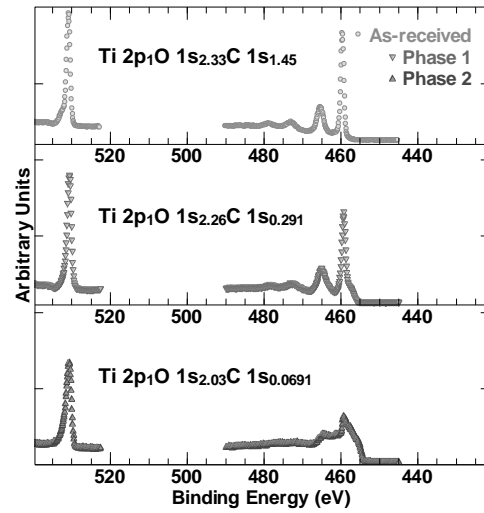
(c)



(d)



(e)



(f)

Figure 1. Spectra collected from a TiO_2 film on Si wafer where XPS narrow scan spectra are collected following sputter cycles using 500 eV argon ions. Evolution of a) Ti 2p, b) O 1s, c) C 1s and d) Ti 3p, O 2s and valence band spectra induced by the ion beam. e) Profile of atomic concentration vs. sputter time. f) Spectral component spectra computed by Principal Component Analysis (PCA) and linear algebraic manipulation of spectra (LAMS) using CasaXPS [17]. Proportions of titanium, oxygen and carbon are computed from the corresponding Ti 2p, O 1s and C 1s spectral shapes within these component spectra.

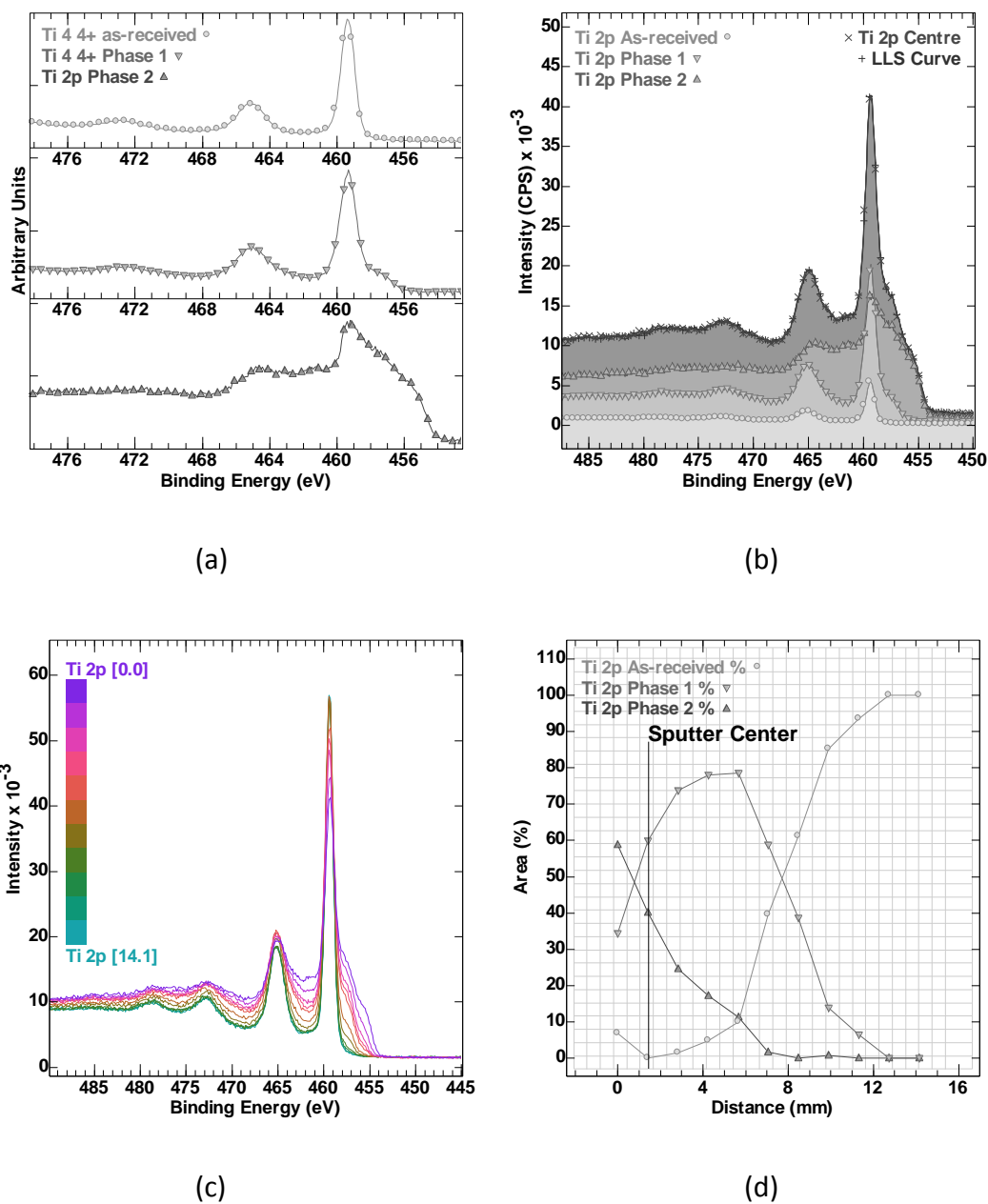
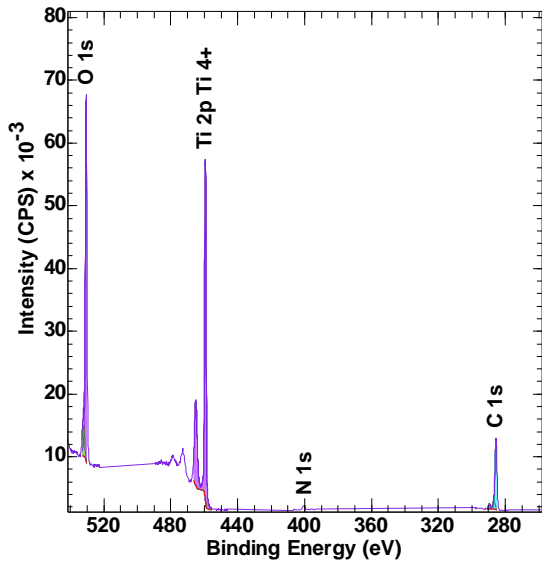
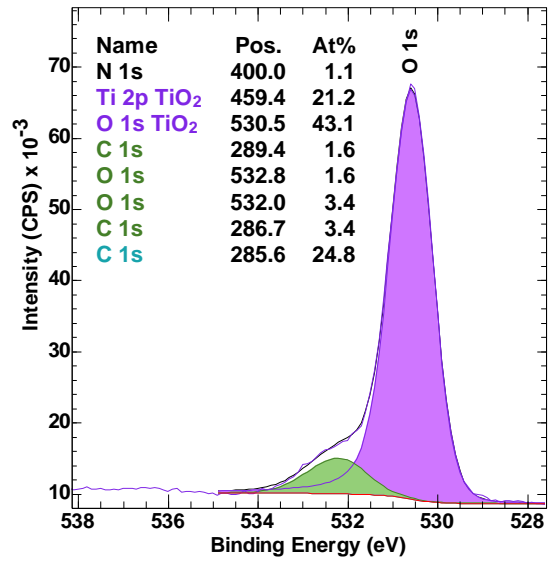


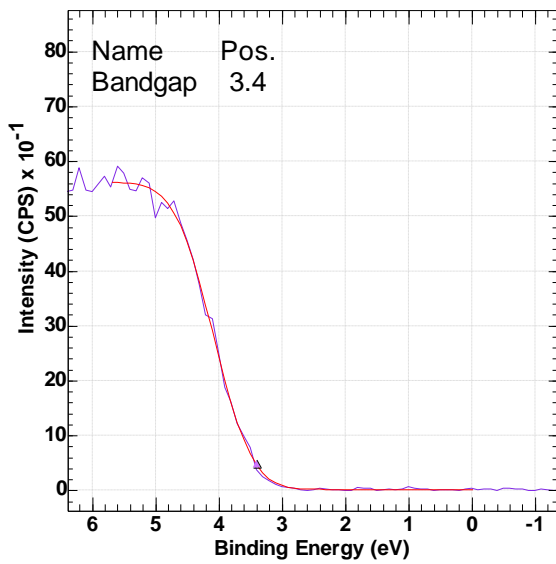
Figure 2. Ti 2p spectra collected along a stage-movement line scan of analysis positions fitted with three Ti 2p component spectra, the shape of which is constructed using data in Figure 1. a) Ti 2p component spectra constructed by analysis of data described in Figure 1. b) An example of a fit of the component-spectra in (a) to a spectrum selected from Ti 2p spectra shown in (c). c) Ti 2p spectra showing the evolution in Ti 2p shape because of changing analysis position along a line from the middle of the sputter-affected sample to locations where the influence of the ion beam is minimal. d) Line scans calculated from peak areas of different phases, characterized by the component spectra in (a), of the sample stimulated by ion beam sputtering.



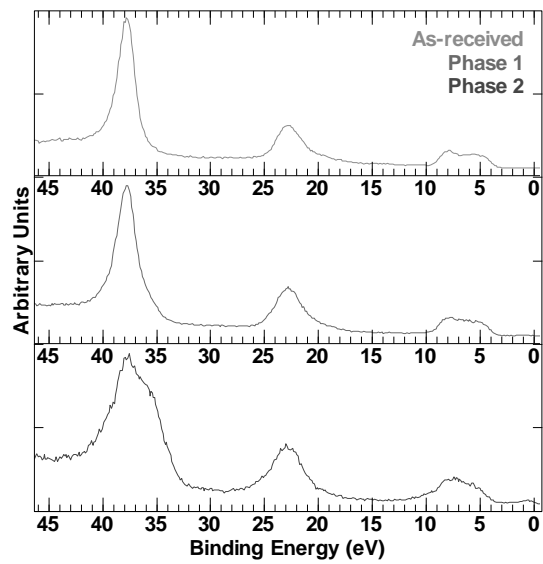
(a)



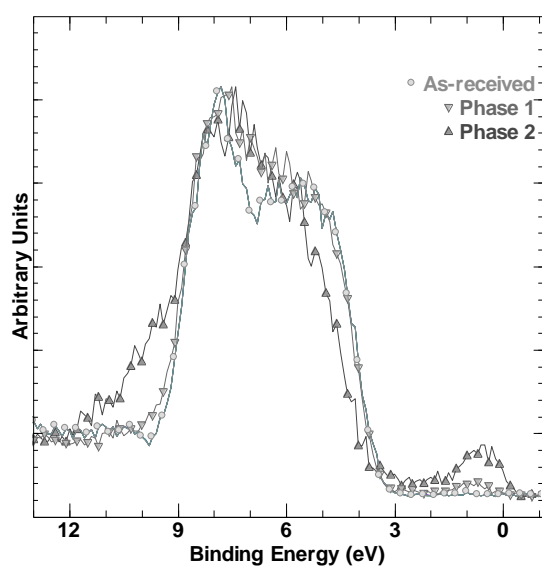
(b)



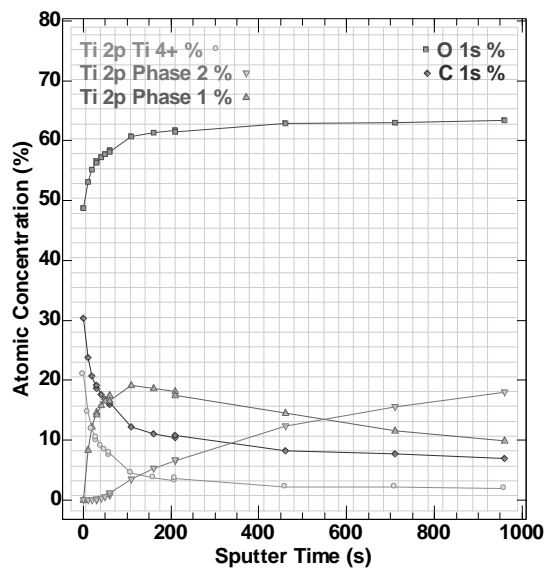
(c)



(d)



(e)



(f)

Figure 3. Quantification of the as-received sample demonstrates, through the fitting of components, the feasibility of the TiO_2 assignment. (a) Narrow scan spectra merged to form vectors corresponding to O 1s, Ti 2p, N 1s, C 1s and valence band (shown in (c)). (b) O 1s narrow scan spectrum corresponding to data shown in (a) fitted with Voigt line shapes. The quantification table specifically illustrates that the oxygen signal can be correlated with the carbon signal, which, once the O 1s signal is correlated with the Ti 2p signal, the expected 2:1 stoichiometry for O:Ti in TiO_2 is recovered. (c) Valence band data corresponding to data in (a) illustrates that the onset of the signal associated with band structures in the as-received sample is compatible with titanium in a 4+ oxidation state. (d) Ti 3p, O 2s and valence band component spectra correspond to deeper core-level photoemission shown in Figure 1f. (e) Valence band spectra corresponding to the component spectra are shown in Figure 1f. (f) Profile of sample changes induced by sputtering equivalent to the profile in Figure 1e, where the three phases of titanium are separated to show the dependence of phase creation on sputter time. Initially, the sputter cycles were of a duration of 10 seconds, during which Phase 2 changes did not occur. Only when the sputter time is increased to 50 seconds per sputter cycle does Phase 2 begin to change. Increasing the sputtering time to 250 seconds per sputter cycle serves to continue the trend of increasing Phase 2 contributions to spectra.

Acknowledgments

This work by J.B. was supported as part of UNCAGE-ME, an Energy Frontier Research Center funded by the U.S. Department of Energy, Office of Science, Basic Energy Sciences under Award No. DE-SC0012577. The CNRS is acknowledged for financial support to the Thematic Workshop (N° 1317144) held at the Station Biologique, Roscoff, France. D.M. acknowledges EPSRC National Facility for XPS ('HarwellXPS') operated by Cardiff University and UCL under contract No. PR16195.

Author contributions

Pascal Bargiela: Investigation (lead); Writing – review and editing (equal). Vincent Fernandez Bargiela: Investigation (lead); Writing – review and editing (equal). William Ravisy: Investigation (lead). David Morgan: Investigation (lead); Writing – review and editing (equal). Mireille Richard-Plouet: Writing – review and editing (equal). Neal Fairley: Conceptualization (lead); Investigation (supporting); Methodology (lead); Writing – original draft (equal); Writing – review and editing (equal). Jonas Baltrusaitis: Conceptualization (lead); Investigation (supporting); Methodology (supporting); Supervision (lead); Writing – original draft (equal); Writing – review and editing (equal).

Competing interests

The authors declare no competing interests.

References

1. Shard, A.G. (2020) Practical guides for x-ray photoelectron spectroscopy: Quantitative XPS. *J. Vac. Sci. Technol. A*, **38** (4), 041201.
2. Cumpson, P.J., Seah, M.P., and Spencer, S.J. (1998) The calibration of Auger and X-ray photoelectron spectrometers for valid analytical measurements. *Spectrosc. Eur.*, **10** (3), 8–15.
3. Seah, M.P. (2012) Simple universal curve for the energy-dependent electron attenuation length for all materials. *Surf. Interface Anal.*, **44** (10), 1353–1359.
4. Reed, B.P., Cant, D.J.H., Spencer, S.J., Carmona-Carmona, A.J., Bushell, A., Herrera-Gómez, A., Kurokawa, A., Thissen, A., Thomas, A.G., Britton, A.J., Bernasik, A., Fuchs, A., Baddorf, A.P., Bock, B., Theilacker, B., Cheng, B., Castner, D.G., Morgan, D.J., Valley, D., Willneff, E.A., Smith, E.F., Nolot, E., Xie, F., Zorn, G., Smith, G.C., Yasufuku, H., Fenton, J.L., Chen, J., Counsell, J.D.P., Radnik, J., Gaskell, K.J., Artyushkova, K., Yang, L., Zhang, L., Eguchi, M., Walker, M., Hajdyla, M., Marzec, M.M., Linford, M.R., Kubota, N., Cortazar-Martínez, O., Dietrich, P., Satoh, R., Schroeder, S.L.M., Avval, T.G., Nagatomi, T., Fernandez, V., Lake, W., Azuma, Y., Yoshikawa, Y., and Shard, A.G. (2020) Versailles Project on Advanced Materials and Standards interlaboratory study on intensity calibration for x-ray photoelectron spectroscopy instruments using low-density polyethylene. *J. Vac. Sci. Technol. A*, **38** (6), 063208.
5. Shard, A.G., Counsell, J.D.P., Cant, D.J.H., Smith, E.F., Navabpour, P., Zhang, X., and Blomfield, C.J. (2019) Intensity calibration and sensitivity factors for XPS instruments with monochromatic Ag L α and Al K α sources. *Surf. Interface Anal.*, **51** (7), 763–773.
6. Ravisy, W., Richard-Plouet, M., Dey, B., Bulou, S., Choquet, P., Granier, A., and Goullet, A. (2021) Unveiling a critical thickness in photocatalytic TiO₂ thin films grown by plasma-enhanced chemical vapor deposition using real time in situ spectroscopic ellipsometry. *J. Phys. D: Appl. Phys.*, **54** (44), 445303.
7. Fernandez, V., Morgan, D., Bargiela, P., Fairley, N., and Baltrusaitis, J. (2023) Combining PCA and nonlinear fitting of peak models to re-evaluate C 1s XPS spectrum of cellulose. *Appl. Surf. Sci.*, **614**, 156182.
8. Garland, B.M., Fairley, N., Strandwitz, N.C., Thorpe, R., Bargiela, P., and Baltrusaitis, J. (2022) A study of in situ reduction of MoO₃ to MoO₂ by X-ray Photoelectron Spectroscopy. *Appl. Surf. Sci.*, **598**, 153827.
9. Béchu, S., Richard-Plouet, M., Fernandez, V., Walton, J., and Fairley, N. (2016) Developments in numerical treatments for large data sets of XPS images. *Surf. Interface Anal.*, **48** (5), 301–309.
10. Bargiela, P., Fernandez, V., Cardinaud, C., Walton, J., Greiner, M., Morgan, D., Fairley, N., and Baltrusaitis, J. (2021) Towards a reliable assessment of charging effects during surface analysis: Accurate spectral shapes of ZrO₂ and Pd/ZrO₂ via X-ray Photoelectron Spectroscopy. *Appl. Surf. Sci.*, **566**, 150728.
11. Major, G.H., Fernandez, V., Fairley, N., Smith, E.F., and Linford, M.R. (2022) Guide to XPS data analysis: Applying appropriate constraints to synthetic peaks in XPS peak fitting. *J. Vac. Sci. Technol. A*, **40** (6), 063201.
12. Major, G.H., Fairley, N., Sherwood, P.M.A., Linford, M.R., Terry, J., Fernandez, V., and Artyushkova, K. (2020) Practical guide for curve fitting in x-ray photoelectron spectroscopy. *J. Vac. Sci. Technol. A*, **38** (6), 061203.
13. Morgan, D.J. (2015) Resolving ruthenium: XPS studies of common ruthenium materials. *Surf. Interface Anal.*, **47** (11), 1072–1079.
14. Scanlon, D.O., Watson, G.W., Payne, D.J., Atkinson, G.R., Egdell, R.G., and Law, D.S.L. (2010) Theoretical and Experimental Study of the Electronic Structures of MoO₃ and MoO₂. *J. Phys. Chem. C*, **114** (10), 4636–4645.
15. Biesinger, M.C., Payne, B.P., Grosvenor, A.P., Lau, L.W.M., Gerson, A.R., and Smart, R.S.C.

- (2011) Resolving surface chemical states in XPS analysis of first row transition metals, oxides and hydroxides: Cr, Mn, Fe, Co and Ni. *Appl. Surf. Sci.*, **257** (7), 2717–2730.
16. Shirley, D.A. (1972) High-Resolution X-Ray Photoemission Spectrum of the Valence Bands of Gold. *Phys. Rev. B*, **5** (12), 4709–4714.
 17. Fairley, N., Fernandez, V., Richard-Plouet, M., Guillot-Deudon, C., Walton, J., Smith, E., Flahaut, D., Greiner, M., Biesinger, M., Tougaard, S., Morgan, D., and Baltrusaitis, J. (2021) Systematic and collaborative approach to problem solving using X-ray photoelectron spectroscopy. *Appl. Surf. Sci. Adv.*, **5**, 100112.
 18. Bauer, F.L., Householder, A.S., Wilkinson, J.H., and Reinsch, C. (2012) *Handbook for Automatic Computation: Volume II: Linear Algebra*, Springer, Berlin Heidelberg.
 19. Cottineau, T., Rouet, A., Fernandez, V., Brohan, L., and Richard-Plouet, M. (2014) Intermediate band in the gap of photosensitive hybrid gel based on titanium oxide: role of coordinated ligands during photoreduction. *J. Mater. Chem. A*, **2** (29), 11499–11508.